JACS
JOURNAL OF THE AMERICAN CHEMICAL SOCIETY

Article

pubs.acs.org/JACS

Monitoring Chemical and Biological Electron Transfer Reactions with a Fluorogenic Vitamin K Analogue Probe

Mei-Ni Belzile, Robert Godin, Andrés M. Durantini, and Gonzalo Cosa*

Department of Chemistry and Center for Self-Assembled Chemical Structures, McGill University, 801 Sherbrooke Street West, Montréal, Québec H3A 0B8, Canada

Supporting Information

ABSTRACT: We report herein the design, synthesis, and characterization of a two-segment fluorogenic analogue of vitamin K, **B-VK$_Q$**, prepared by coupling vitamin K$_3$, also known as menadione (a quinone redox center), to a boron-dipyrromethene (BODIPY) fluorophore (a lipophilic reporter segment). Oxidation–reduction reactions, spectroelectrochemical studies, and enzymatic assays conducted in the presence of DT-diaphorase illustrate that the new probe shows reversible redox behavior on par with that of vitamin K, provides a high-sensitivity fluorescence signal, and is compatible with biological conditions, opening the door to monitor remotely (i.e., via imaging) redox processes in real time. In its oxidized form, **B-VK$_Q$** is non-emissive, while upon reduction to the hydroquinone form, **B-VK$_{QH_2}$**, BODIPY fluorescence is restored, with emission quantum yield values of *ca.* 0.54 in toluene. Density functional theory studies validate a photoinduced electron transfer intramolecular switching mechanism, active in the non-emissive quinone form and deactivated upon reduction to the emissive dihydroquinone form. Our results highlight the potential of **B-VK$_Q$** as a fluorogenic probe to study electron transfer and transport in model systems and biological structures with optimal sensitivity and desirable chemical specificity. Use of such a probe may enable a better understanding of the role that vitamin K plays in biological redox reactions ubiquitous in key cellular processes, and help elucidate the mechanism and pathological significance of these reactions in biological systems.

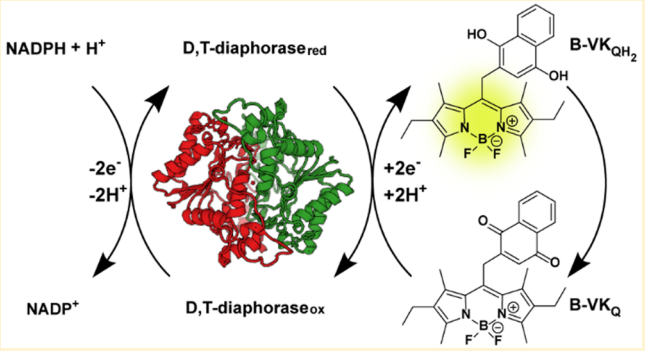

INTRODUCTION

Electron transport within cell membranes is a most fundamental chemical process in living systems, involved in cellular respiration and in photosynthesis. Deficiencies in electron transport during respiration are associated with a number of pathologies and the onset of oxidative stress and reactive oxygen species generation.[1,2] Electron transport requires interplay between a number of protein complexes and their associated redox cofactors, and for membrane-embedded mobile carriers acting as electron relay systems to transport electrons between complexes along the lipid membrane.[3−5] Carriers may involve a quinone/dihydroquinone redox couple operating via proton-coupled electron transfer (PCET) reactions.[6]

Ubiquitously found in Nature, compounds within the vitamin K family[7] which bear a 2-methyl-1,4-naphthoquinone core and a variety of alkyl tails (Figure 1) act as electron carriers in bacterial cellular respiration[8,9] and in the photosynthetic membrane.[10,11] Vitamin K$_2$ has further been shown to serve as a mitochondrial electron carrier in *Drosophila*.[9] Additionally, vitamin K is an important cofactor in blood coagulation in mammals,[8,12] where it plays a pivotal role as a redox relay molecule in the γ-carboxylation of specific glutamate residues in vitamin K-dependent proteins.[13,14]

Given its critical role in living systems, non-invasive imaging methodologies able to monitor real-time and *in situ* vitamin K redox and transport properties are highly desirable. A fluorogenic probe[15−21] capable of reporting via emission enhancement changes in the redox status of vitamin K is essential toward gaining a mechanistic understanding of vitamin K's physiological role. This probe, when coupled with state-of-the-art microscopy imaging technologies, will make it possible to interrogate the redox status of biological systems with high spatiotemporal resolution. Such a tool will offer the opportunity to correlate electron transport activity with cell homeostasis, and to develop diagnostics of mitochondrion activity and mitochondrial diseases associated with deficiencies in electron transport. Ultimately, a fluorogenic vitamin K analogue may shed light on the overall impact of this vital carrier in sustaining cell viability.

Building on our own experience in preparing lipophilic fluorogenic probes, including α-tocopherol[21−24] analogues and a recent ubiquinone[25] analogue, here we report the design, synthesis, and characterization of a fluorogenic probe, **B-VK$_Q$** (Figure 1C), which mimics vitamin K in structure and activity.

Received: September 16, 2016
Published: November 22, 2016

DOI: 10.1021/jacs.6b09735
J. Am. Chem. Soc. 2016, 138, 16388−16397

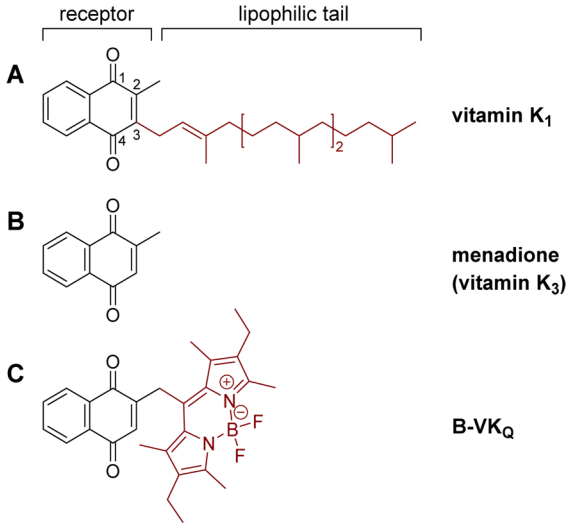

Figure 1. Structures of (A) the natural form of lipophilic vitamin K_1, (B) menadione (also known as vitamin K_3), and (C) the fluorogenic vitamin K analogue, **B-VK$_Q$**, reported herein.

B-VK$_Q$ is a two-segment receptor–reporter probe[26] consisting of the redox-sensitive menadione moiety (2-methyl-1,4-naphthoquinone, vitamin K_3) coupled to the *meso* position of a boron-dipyrromethene (BODIPY) fluorophore via a methylene linker. The probe relies on intramolecular photoinduced electron transfer (PeT) from the BODIPY moiety (reporter) to the naphthoquinone segment (receptor) to impart an off–on fluorescence switch. In the oxidized form, **B-VK$_Q$** is completely non-emissive. Upon reduction of the menadione segment to menadiol, the highly emissive dihydroquinone form of the probe **B-VK$_{QH_2}$** is generated, with an emission quantum yield Φ_f of *ca.* 0.54. The menadione–BODIPY adduct emulates the redox properties and chemical reactivities of vitamin K species, preserving their lipophilic character and preferential lipid partitioning, while yielding a highly sensitive, reversible redox probe.[19] The probe reports a two-electron and two-proton reduction via dramatic emission enhancement in not only nonpolar but also polar solvents such as acetonitrile. In this regard, **B-VK$_Q$** amply surpasses the sensitivity performance of a recently published fluorogenic analogue of ubiquinone,[25] characterized by a slightly lower redox potential.

Oxidation–reduction reactions, spectroelectrochemical studies with trace amounts of compound, and enzymatic assays conducted in the presence of DT-diaphorase illustrate that the new probe shows reversible redox behavior on par with that of vitamin K, provides a high sensitivity fluorescence signal, and is compatible with biological conditions. The new probe opens the door to monitor remotely (i.e., via imaging) redox processes in real time, and potentially at the single molecule level.

RESULTS AND DISCUSSION

Design of B-VK$_Q$. In order to provide chemical specificity and redox reversibility characteristic of vitamin K, we selected the menadione moiety as the receptor segment. A BODIPY chromophore was used as the reporter segment. BODIPYs have optimal spectroscopic properties, and their lipophilic nature enables substitution of the alkyl tails of vitamin K_1 and K_2 for the dye without altering the lipid partitioning (Figure 1). BODIPY fluorophores are also amenable to synthetic modifications to tune their redox properties.[27,28] PeT may then be exploited to switch the probe emission.[21,26,29] By tuning the BODIPY segment only while preserving intact the receptor (vitamin K) segment, we ensured that the intrinsic chemical properties of the latter would be retained.[23,24] Together, the redox-active menadione segment and the judiciously chosen lipophilic fluorescent segment rendered a fluorogenic analogue of vitamin K.

To ensure that PeT from the BODIPY to the naphthoquinone segment would be exergonic[30] (non-emissive) in the

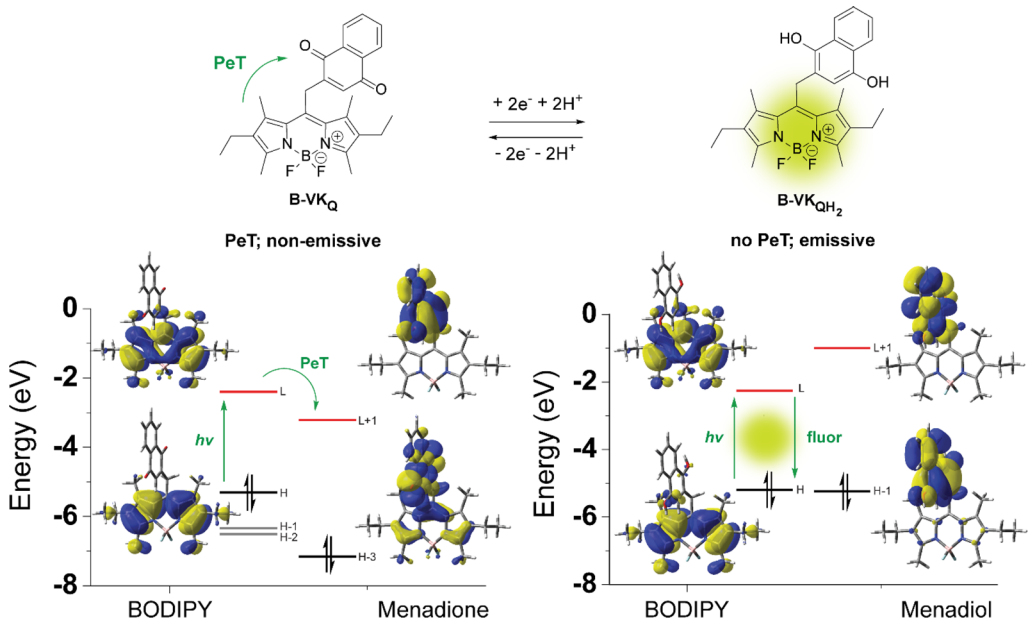

Figure 2. Off–on fluorogenic mechanism of **B-VK$_Q$** based on PeT. HOMO (black line) and LUMO (red line) energy levels for receptor (vitamin K) and reporter (BODIPY) moieties of the oxidized and reduced forms of the **B-VK$_Q$** probe as calculated computationally using the B3LYP 6-31g(d) level of theory without a solvent model.

DOI: 10.1021/jacs.6b09735
J. Am. Chem. Soc. 2016, 138, 16388–16397

Scheme 1. Preparation of B-VK$_Q$

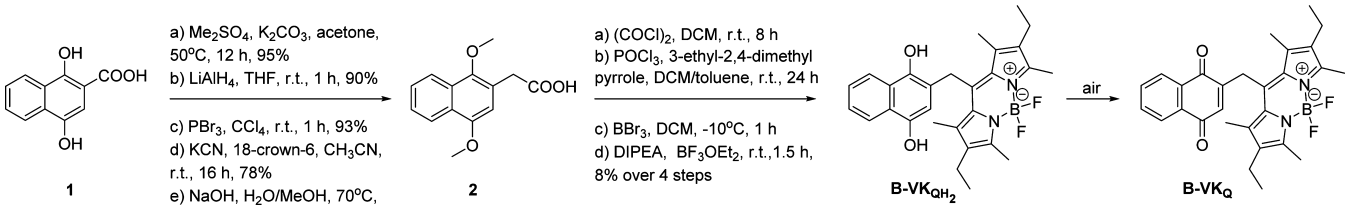

Table 1. Spectroscopic Properties of B-VK$_{QMe_2}$, B-VK$_Q$, and B-VK$_{QH_2}$ in Different Solvents

compound	solvent	λ_{max} (nm) Abs	λ_{max} (nm) Em	ε ($\times 10^3$ M^{-1} cm^{-1})	Φ_f[a]	k_{dec} ($\times 10^7$ s^{-1})	k_{rad} ($\times 10^7$ s^{-1})	k_{nr} ($\times 10^7$ s^{-1})
B-VK$_{QMe_2}$	MeCN	523	538	38[c]	0.16 ± 0.01	68.9	11.0	57.9
	toluene	528	540	80	0.87 ± 0.02	18.4	16.2	2.2
B-VK$_Q$	MeCN	525	544	21[c]	0.00070 ± 0.00002	–[b]	–[b]	–[b]
	toluene	532	546	75	0.0006 ± 0.0002	–[b]	–[b]	–[b]
B-VK$_{QH_2}$	MeCN	522	536	35 ± 1[d,e]	0.0400 ± 0.0001[d,e]	142.8[d,e]	5.7	137.1
	toluene	529	541	85 ± 5[e]	0.54 ± 0.05[e]	21.1[e]	11.4	9.7

[a]Quantum yields were measured using PM605 as a standard (ϕ_f = 0.72 and 0.89 in acetonitrile and toluene, respectively).[36] [b]Not available. [c]Although we do not fully understand the cause of the substantial decrease in extinction coefficient in acetonitrile, it is possible that aggregation and subsequent distortions to the electronic structure are at play. [d]Spectroscopic measurements of B-VK$_{QH_2}$ in acetonitrile were performed by carrying out *in situ* reduction of B-VK$_Q$ with sodium borohydride in toluene and then diluting a 10 μL aliquot of this reaction mixture in 3 mL of acetonitrile. The direct reduction in acetonitrile led to undesired BODIPY decomposition (Figure S7). [e]We assume the *in situ* reduction achieves almost complete conversion to the hydroquinone form B-VK$_{QH_2}$, and thus the amount of starting B-VK$_Q$ is negligible.

oxidized form of the naphthoquinone/menadione segment but endergonic (emissive) in its reduced form, we chose electron-releasing alkyl groups to decorate the BODIPY core. These groups raise both the HOMO and LUMO of the BODIPY segment, enhancing the feasibility of PeT from the BODIPY to naphthoquinone while preventing PeT from the HOMO of the reduced form of naphthoquinone to the BODIPY core.[30] Density functional theory (DFT) calculations at the B3LYP 6-31g(d) level of theory[31] confirmed that alkyl group substitution on the BODIPY core satisfied these criteria, rendering a dark compound in its oxidized form and an emissive one following reduction; see Figure 2. Additionally, alkyl substitution in BODIPY dyes increases their lipophilic character.[32]

In order to retain high lipophilicity, maximize structural similarity to menadione, and minimize the distance between the vitamin K and BODIPY moieties, while ensuring competitive PeT in the oxidized form, a short aliphatic methylene bridge was incorporated in the design.[23]

Synthesis of B-VK$_Q$. We used the commercially available 1,4-dihydroxy-2-naphthoic acid (**1**) as the precursor of the vitamin K/menadione receptor segment. To introduce the methylene linker between the menadione and BODIPY segments, the aliphatic chain of the starting carboxylic acid **1** had to be extended by one carbon (Scheme 1). After protection of the sensitive hydroxyl groups, the methyl ester functionality was reduced to an alcohol and then replaced with a bromine atom. Substitution by a nitrile and hydrolysis under basic conditions yielded the desired carboxylic acid, 1,4-dimethoxy-2-methylnaphthoic acid (**2** in Scheme 1). The acid chloride of **2** was then prepared and reacted with 2 equiv. of 3-ethyl-2,4-dimethylpyrrole in the presence of phosphorus oxychloride. Pyrrole condensation gave the dipyrrin bearing the desired vitamin K substituent at the *meso* position. Subsequent deprotection with BBr_3, followed by addition of DIPEA and $BF_3{\cdot}OEt_2$, gave the desired B-VK$_Q$ probe in 8% overall yield, starting from compound **2**. (Since the deprotected hydroquinone rapidly oxidizes in air, we obtained the probe, B-VK$_Q$, in the quinone form.) The methyl-protected form of the probe, B-VK$_{QMe_2}$, was also obtained by simply omitting the deprotection step with BBr_3 (Scheme 1).

Spectroscopic and Electrochemical Properties of B-VK$_Q$. The absorption and fluorescence spectroscopic properties of B-VK$_Q$, B-VK$_{QH_2}$, and B-VK$_{QMe_2}$ are presented in Table 1 (see Figure S1 for structures and Figure S2 for spectra). While the quinone form is non-emissive regardless of the solvent, both the hydroquinone and methoxy-protected forms are emissive, with quantum yields 5−10-fold smaller in acetonitrile than in toluene. In turn, time-resolved fluorescence experiments revealed that the decay rate constant k_{dec} of the excited sate is 3−7-fold faster in the more polar solvent, primarily caused by a larger non-radiative rate constant; see Table 1. The increase in non-radiative decay may be attributed to an intramolecular quenching pathway, presumably photo-induced reduction of the BODIPY chromophore by the dihydroquinone moiety or its methyl ether form, as evidenced by the proximity in energy of the BODIPY and dihydroquinone HOMOs (Figure 2). This process is facilitated in polar (e.g., acetonitrile) solvents.[33,34]

In order to show the electrochemical reversibility of the B-VK$_Q$/B-VK$_{QH_2}$ redox couple, cyclic voltammetry (CV) was next performed in dry acetonitrile and subsequently in the presence of 10.8 M water; see Table S1 for a list of the redox potentials recorded.

In aprotic conditions (specifically in dry acetonitrile which likely contains traces of water), we observed two cathodic peaks in the CV experiment for B-VK$_Q$: a first reversible peak at

DOI: 10.1021/jacs.6b09735
J. Am. Chem. Soc. 2016, 138, 16388−16397

−0.40 V and a second quasi-reversible peak at −1.00 V vs NHE (Figure 3A, showing 6 scans). The first peak, at −0.40 V, was

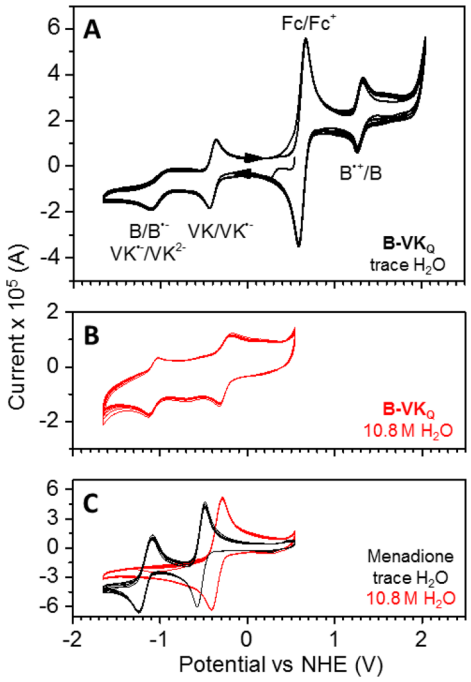

Figure 3. (A) Cyclic voltammogram (6 scans) for **B-VK$_Q$** (1 mM) in argon-purged dry acetonitrile solution (likely with traces of water) containing 0.1 M Bu_4NPF_6. The Fc^+/Fc (1 mM) redox couple was used as an internal standard. (B) CV for **B-VK$_Q$** (6 scans) recorded with 10.8 M water under otherwise identical experimental conditions. (C) CV for menadione (6 scans) recorded under trace water conditions (black) or 10.8 M water (red). All other conditions were as above.

assigned to the first reduction of the naphthoquinone segment to its semiquinone radical anion form, consistent with literature values for the first standard reduction potential for menadione, given as $E^{o}_{Q/Q^{\bullet-}} = -0.41$ V vs NHE (in DMF and acetonitrile),[35] and also consistent with the value of −0.53 V we recorded in acetonitrile (*vide infra*).

The second peak was assigned to a complex reduction of the coupled BODIPY core and quinone moiety. The redox potential recorded herein is similar to the reported value for an analogous ethyl-substituted BODIPY ($E^{o}_{B/B^{\bullet-}} = -1.21$ V vs NHE in acetonitrile).[30,36] The cathodic peak at −1.00 V may also contain a contribution from the reduction of the semiquinone radical anion to the deprotonated dihydronaphthoquinone **B-VK$_Q^{2-}$**, consistent with literature values reporting $E^{o}_{Q^{\bullet-}/Q^{2-}} = -1.14$ V vs NHE for menadione in DMF and acetonitrile[35] and consistent with our own value of −1.16 V recorded in acetonitrile (*vide infra*). We also observed reversible oxidation of the BODIPY moiety at 1.29 V, further consistent with previous reports ($E^{o}_{B^{\bullet+}/B} = 1.23$ V vs NHE in acetonitrile).[30,36] The redox potentials of the BODIPY oxidation and reduction of the naphthoquinone, combined with the E_{00} value obtained from steady-state optical spectroscopy, allow us to calculate a PeT driving force of −0.78 eV (see Supporting Information). Comparing this to the calculated value of −0.82 eV confirms our expectations and supports the initial assessment of probe design by computational methods.

To better establish the origin of the peaks and their reversible nature, we next conducted CV experiments under protic conditions (see Figure 3B). It has been shown for the electrochemistry of vitamin K in acetonitrile, and quinones in general, that addition of water or acid results in the coalescence of the first and second one-electron reduction peaks recorded under anhydrous aprotic conditions into a single two-electron reduction peak shifted to less negative bias.[37−39]

Experiments conducted with **B-VK$_Q$** in acetonitrile supplemented with 10.8 M water showed two reversible peaks at −0.27 and −1.08 V. The data are consistent with a shift toward more positive values for the reduction potential of the naphthoquinone moiety. They are also consistent with a decoupling of the reduction potential of the BODIPY core, as exemplified by both the reversible nature of the second peak and its shift toward more negative values (rather than a shift to positive values as would have been expected for the second reduction potential of the naphthoquinone moiety after addition of water). Furthermore, a reversible BODIPY core reduction at −0.97 V was observed with **B-VK$_{QMe_2}$** (Figure S3), supporting that the quasi-reversible nature of the −1.00 V redox process seen for **B-VK$_Q$** under aprotic conditions can be attributed to coupling of the BODIPY and quinone moieties.

While we anticipated the first reduction wave in Figure 3B to integrate for a two-electron process under protic conditions, the CV intensity prevented clear integrations from being made. Here both reduction waves showed similar peak intensities. Control experiments performed with menadione showed that two reversible peaks originally observed in dry acetonitrile (with trace H_2O) at −0.53 and −1.16 V coalesced into one peak at −0.35 V in the presence of 10.8 M water; see Figure 3C. The new wave for menadione is significantly broadened, integrating for twice as much as either of the two reversible waves recorded under trace H_2O conditions. Arguably, a similar peak broadening was also experienced with **B-VK$_Q$** under protic conditions.

We may conclude that electrochemical processes of **B-VK$_Q$** are reversible in protic media. Importantly, the similar redox potentials and shifts of the vitamin K CV waves in **B-VK$_Q$** and menadione after the addition of water indicate that the desired redox behavior of menadione is conserved in the probe.

Chemical Reduction. In order to validate the fluorogenic nature of **B-VK$_Q$**, we first carried out a chemical reduction of the menadione segment with H_2 using palladized charcoal and cyclohexene with methanol as a source of protons. After 18 h, the reaction yielded a fluorescent product, determined to be the reduced form of the probe by both ^{1}H NMR and high-resolution mass spectrometry (Figures S4 and S5). Since hydroquinones oxidize rapidly in air,[40] the characterization methods showed the presence of both the reduced and oxidized forms of the probe, precluding an exact determination of the reaction yield.

We next attempted an *in situ* chemical reduction of the probe in a cuvette using sodium borohydride,[41] to minimize oxidation prior to analysis. A solution of **B-VK$_Q$** (1.2 μM in toluene) was reduced at room temperature with sodium borohydride (1 mg/mL) and a small amount of water (1 μL/mL), acting as a hydrogen-bonding source. An increasing fluorescence intensity with time was observed and was periodically monitored under photoexcitation at 503 nm. The fluorescence intensity plateaued after 10 min of reaction, displaying a greater than 1000-fold fluorescence enhancement once the insoluble sodium borohydride was filtered out (Figure 4). The emission spectra obtained under both reduction conditions showed a good

DOI: 10.1021/jacs.6b09735
J. Am. Chem. Soc. 2016, 138, 16388−16397

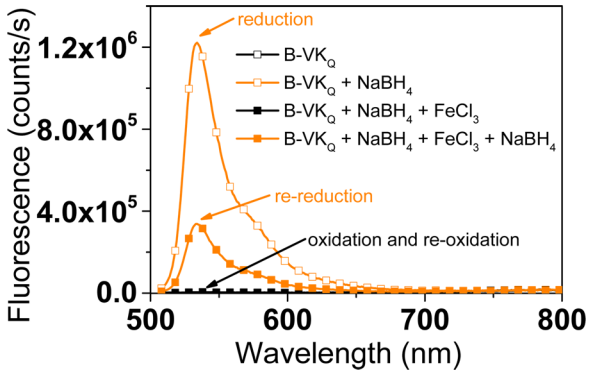

Figure 4. Emission spectrum of **B-VK$_Q$** (1.2 μM in toluene, argon equilibrated) before (black □) and after reduction by sodium borohydride (orange □), subsequent re-oxidation using 300 μM $FeCl_3$ (black ■), and final reduction using $NaBH_4$ (orange ■).

overlap (Figure S8). Absorption spectra before and after reaction with $NaBH_4$ further show a slight shift in λ_{max} (Figure S6). In order to show the reversibility of the probe, the cuvette solution was next oxidized by adding 300 μM $FeCl_3$[42] in order to reconvert **B-VK$_{QH_2}$** to initial non-emissive **B-VK$_Q$**. The fluorescence decreased to that of pristine **B-VK$_Q$**, confirming oxidation and redox reversibility. Finally, the $NaBH_4$ reduction was repeated a final time in order to show that the probe can return to its emissive state after oxidation. The fluorescence once again increased after a few minutes, reaching a third of the maximum fluorescence intensity achieved in the first reduction. It is plausible that filtrations after every step reduced the amount of probe in solution, leading to this drop in intensity, or the intensity reduction indicates chemical degradation caused by the strong redox agents used.

Fluorescence Spectroelectrochemistry. In order to correlate applied redox potential with emission intensity for **B-VK$_Q$** upon its electrochemical reduction, we turned to fluorescence microscopy-based spectroelectrochemistry (SEC), a powerful tool that allows for monitoring trace amounts of fluorescent molecules under electrochemical control.[43−47] SEC experiments were performed on a confocal microscope setup to enable visualization of newly generated fluorescent compounds (Figure 5A). An electrochemical cell was custom-built by gluing a glass tube on top of a coverslip coated with optically transparent platinized ITO (working electrode). In our studies, the fluorescent products were generated under the direct reduction of 500 nM **B-VK$_Q$** (in dry acetonitrile, may contain trace H_2O) in the presence of acetic acid as a proton source, in order to produce the fluorescent hydroquinone form **B-VK$_{QH_2}$** (Figure 5B).

The intensity−time trajectory vs applied bias recorded for **B-VK$_Q$** in the presence of acetic acid displayed a rapid rise in fluorescence intensity with potentials more negative than −0.35 V vs NHE (red trace in Figure 5D) upon scanning the potential over time (20 mV/s) toward negative bias (Figure 5C). We assign the intensity rise to the formation of **B-VK$_{QH_2}$**. A maximum fluorescence intensity was reached at a potential of −0.57 V, going from an initial average 2.4 counts/ms at resting potential to an average 124 counts/ms at the maximum,

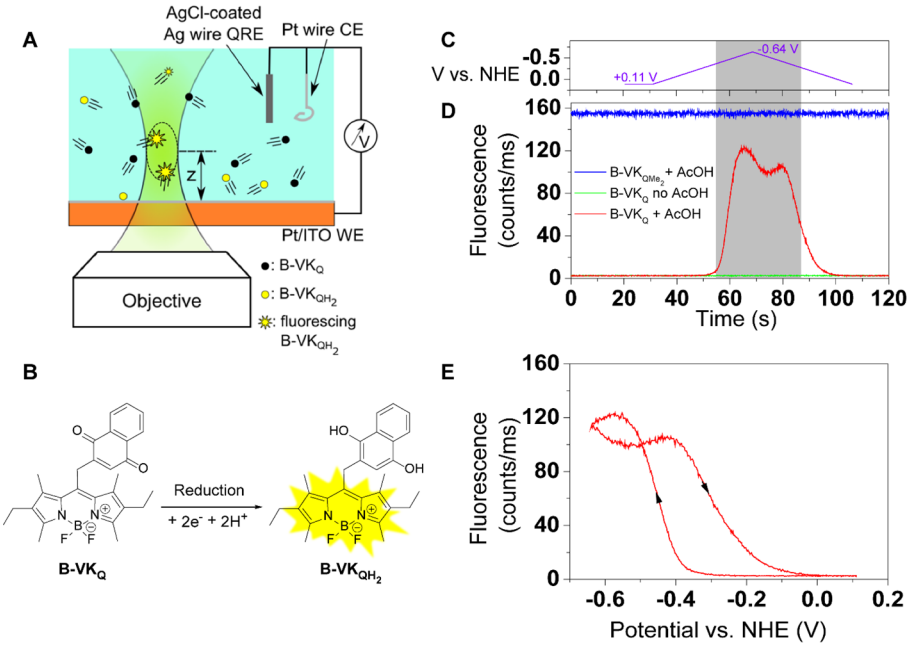

Figure 5. (A) SEC setup depicting **B-VK$_Q$** molecules that are oxidized at the surface of the Pt/ITO working electrode and then diffuse through the confocal observation volume (dotted oval) and emit fluorescence. The distance between the electrode surface and the observation volume was controlled by a piezo nanopositioner. (B) Reduction of **B-VK$_Q$** to yield fluorescent **B-VK$_{QH_2}$**. (C) Applied electrochemical potential. The potential scan rate was 20 mV/s. (D) Fluorescence trajectories of pristine **B-VK$_Q$** with and without the presence of AcOH, and of **B-VK$_{QMe_2}$** (with AcOH) in acetronitrile under the influence of the biases shown in (C). Solutions are argon equilibrated. Times where E_{app} is more negative than −0.35 V are highlighted in gray. The concentration of **B-VK$_Q$** was 500 nM. Trajectories were acquired with the observation volume 20 μm above the electrode surface, and counts were calculated using 100 ms time bins. (E) Change in fluorescence intensity plotted versus the applied potential. Arrows indicate the direction of the potential scan, where the increase in fluorescence occurs as the potential is scanned toward negative potential, and the decrease occurs as the potential is scanned back toward 0 V.

DOI: 10.1021/jacs.6b09735
J. Am. Chem. Soc. 2016, 138, 16388−16397

Scheme 2. Electron Shuttling by B-VK$_Q$/B-VK$_{QH_2}$, Where DT-Diaphorase Catalyzes the Reduction of Cytochrome *c*, Using NADPH as the Electron Donor and Quinones as an Electron Relay System[a]

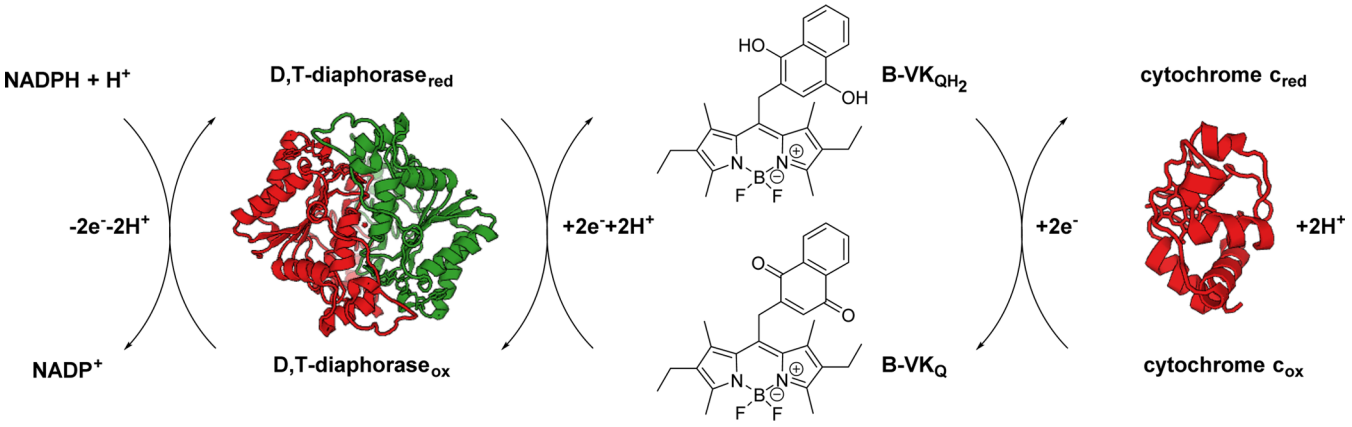

[a]DT-diaphorase and cytochrome *c* structures obtained from the Protein Data Bank (www.rcsb.org):[52] PDB ID 1D4A,[53] and PDB ID 3ZCF, respectively.[54]

yielding a *ca.* 70-fold fluorescence intensity enhancement.[48] The maximum intensity achieved with **B-VK$_Q$** with acetic acid is comparable to that recorded with 500 nM of the control compound **B-VK$_{QMe_2}$** under identical conditions (average 155.0 counts/ms). The latter displayed a bias-insensitive intensity–time trajectory (blue trace in Figure 5D). A control experiment with **B-VK$_Q$** and no acetic acid showed that the intensity remained at background levels versus the applied potential, consistent with the non-emissive character of the **B-VK$_Q^{2-}$** dianion (deprotonated form of **B-VK$_{QH_2}$**) formed under these conditions. Figure S10 compares the initial (at resting potential) and final (at −0.57 V vs NHE) fluorescence intensities and overall intensity enhancements from all SEC experiments, underscoring that a significant enhancement is only observed in the electroreduction of **B-VK$_Q$** under protic conditions.

The maximum enhancement observed was recorded at a significantly less negative reduction potential (−0.57 V) than that observed in the CV experiments for the two-electron reduction of **B-VK$_Q$** in aprotic conditions (peak at −1.00 V). The potential recorded is consistent with the shift toward higher (less negative) values for the second reduction peaks of menadione (−0.37 V) and **B-VK$_Q$** (−0.26 V) recorded in the presence of water (Figure 3).

Sweeping the bias beyond the intensity maximum to more negative bias led to an intensity decrease. This potential is considerably less negative compared to reduction potentials for similar BODIPY analogues and the BODIPY reduction potential observed for **B-VK$_Q$** in the presence of water (Figure 3B).[22,30] Further, no decrease in fluorescence was observed for the **B-VK$_{QMe_2}$** control compound (blue trace in Figure 5D; see Figure S3 for CV). It is possible that hydrogen bonding occurs between **B-VK$_{QH_2}$** and AcOH in the mixture, turning on a new PeT quenching pathway, or that **B-VK$_{QH_2}$** in the presence of AcOH may be easier to reduce than either component through coupling of electronic structure. As the applied potential was scanned back toward 0 V, the fluorescence intensity increased from −0.5 to −0.35 V, consistent with continued reduction of the menadione moiety at these potentials. The increase is also consistent with the end of the fluorescence-quenching reduction that took place at more negative potentials. Note that the oxidation potential of the fluorescent species is expected to shift toward more positive potentials because of protonation of the anionic species originally formed. This results in the slower decay of the fluorescence as compared to the rise (Figure 5E), since the fluorescence decrease is attributed to the diffusion-limited dispersion of fluorescent **B-VK$_{QH_2}$** rather than electrochemical re-oxidation to the non-emissive form.

Altogether, the previous results show that the system **B-VK$_Q$**/**B-VK$_{QH_2}$** provides a reversible and most sensitive fluorescence marker of redox status. Here fluorescence enhancements necessitated the formation of **B-VK$_{QH_2}$**.

Enzymatic Assays. To determine whether the probe is recognized as an enzyme substrate and may act as an electron shuttle in biological systems, we performed enzymatic assays using **B-VK$_Q$** and the enzyme DT-diaphorase, also known as NAD(P)H:quinone oxidoreductase (EC 1.6.99.2).[49] This flavoprotein catalyzes the two-electron reduction of quinones and quinoid compounds (including K vitamins) using either NADPH or NADH as the electron donor.[50,51] DT-diaphorase activity was first determined spectrophotometrically by measuring the increase in absorption at 550 nm upon reduction of cytochrome *c* in the presence of NADPH as an electron source and **B-VK$_Q$** as an electron relay system. Here, **B-VK$_Q$** effectively shuttles electrons from NADPH to cytochrome *c*; see Scheme 2. Control studies with vitamin K$_3$ (menadione) or with no quinones were also conducted to compare the rates of reaction.

The reduction of cytochrome *c* was observed to readily take place with both menadione and **B-VK$_Q$**, while reduction was relatively very slow when no naphthoquinone substrate was added. The rate constant *k* and activity values are listed in Table 2 (see Figure S11 and general procedures in the Supporting Information). All other controls showed no reaction, where we tested every combination of the four components involved in the enzymatic assay: DT-diaphorase, **B-VK$_Q$** (or menadione), cytochrome *c*, and NADPH (Figures S12 and S13). The results are consistent with **B-VK$_Q$** providing a suitable substrate that readily mimics vitamin K$_3$.

Fluorescence monitoring of the DT-diaphorase enzyme-assisted reduction of **B-VK$_Q$** to the dihydroquinone **B-VK$_{QH_2}$**

DOI: 10.1021/jacs.6b09735
J. Am. Chem. Soc. 2016, 138, 16388−16397

Table 2. Activity of DT-Diaphorase with Either Vitamin K_3 (Menadione) or Vitamin K BODIPY Probe (B-VK_Q)

substrate	enzyme activity (nmol min^{-1} mg^{-1})[a,b]	rate constant, k (s^{-1})[b]
menadione	12.35 ± 1.4	0.05 ± 0.01
B-VK_Q	7.66 ± 0.3	0.007 ± 0.001
none	3.23 ± 0.6	0.00008 ± 0.0001

[a]Nanomoles of cytochrome *c* reduced per minute per milligram of enzyme. [b]Values are averages of three replicate experiments with the according standard deviation.

allowed a sensitive visualization of the reaction. The enzymatic assays were carried out under the same conditions as above, without the presence of cytochrome *c*, to prevent regeneration of the oxidized form of the probe. In order to minimize BODIPY aggregation arising from $\pi-\pi$ stacking and hydrophobic interactions in aqueous solution, potentially leading to self-quenching,[55] we conducted the assay in liposomes, with the lipophilic **B-VK_Q** embedded in the bilayer.

In the absence of oxygen, a larger than 30-fold fluorescence intensity enhancement was observed upon the enzymatic reduction of **B-VK_Q**. Control experiments showed no increase in fluorescence in the absence of either **B-VK_Q** or NADPH or DT diaphorase enzyme (Figure S14). Recording the emission spectrum of the enzymatic reduction over time, the appearance of an emission peak at 537 nm was observed, consistent with formation of the reduced **B-VK_{QH_2}** species (Figure S15). These results further support that the **B-VK_Q** probe is compatible with biological systems and may serve as an electron shuttle, working in tandem with proteins.

We note that the smaller sensitivity observed in the liposome studies (30-fold enhancement vs 70-fold and >1000-fold enhancements for SEC and chemical reduction studies, respectively) may be the result of partial probe reduction under the biological conditions explored. The higher polarity of the water−lipid interface where the probe is expected to sit, akin to that in acetonitrile,[56,57] may also result in a smaller emission quantum yield for the probe; see Table 1 and discussion of SEC vs chemical reduction experiments, *vide supra*. Additionally, we note that O_2 leakage may lead to a steady-state condition that results in a lower intensity at the plateau as a result of ongoing regeneration of **B-VK_Q** from **B-VK_{QH_2}**. Consistent with the latter, we recorded a decrease of the fluorescence intensity over time in the enzymatic reduction assay after a plateau was initially reached. Upon degassing with additional argon, the fluorescence intensity was restored, before a new plateau was reached (Figure 6). This confirms that oxygen diffuses back in the system, causing auto-oxidation of the probe, further highlighting its extreme sensitivity to the redox environment.

CONCLUSION

We have shown herein the synthesis and characterization of a two-segment receptor−reporter fluorogenic vitamin K analogue, **B-VK_Q**, a desirable probe to monitor electron transfer and transport in model systems and biological structures. **B-VK_Q** displays reversible turn-on fluorescence upon two-electron and two-proton reduction of the menadione moiety to its menadiol counterpart. It retains the redox specificity and reversibility imparted from the menadione moiety, as validated via a suite of chemical reactions and SEC techniques.[47] Our own SEC studies provide preliminary results in this direction.

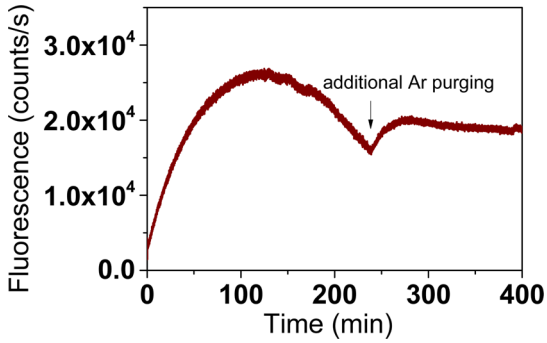

Figure 6. Increase in fluorescence upon enzymatic reduction of **B-VK_Q** by DT-diaphorase. Experiments were conducted after degassing with Ar, where the system was re-purged with argon to remove oxygen at the time indicated by the arrow.

Furthermore, **B-VK_Q** shows high sensitivity, surpassing 1000-fold fluorescence enhancement in nonpolar systems, making it a suitable probe to conduct enzymology studies not only in bulk but also at the single molecule level, where signal-to-background ratios place a stringent constraint on the fluorescent contrast between the off and on forms of a fluorogenic probe. Important for bioimaging considerations, the biological compatibility of our probe was demonstrated upon reactions with DT-diaphorase (a naturally occurring quinone oxidoreductase) and via lipid membrane insertion. Given that the receptor segment preserves intact the electronic moiety of vitamin K_3, we further postulate that **B-VK_Q** may enable a better understanding of the role that vitamin K plays in key biological redox processes, including photosynthesis and cellular respiration, and help elucidate the mechanism and pathological significance of redox reactions in biological systems.

EXPERIMENTAL SECTION

Materials. 8-Acetoxymethyl-2,6-diethyl-1,3,5,7-tetramethylpyrromethene fluoroborate (PM605) was purchased from Exciton, Inc. (Dayton, OH). HPLC-grade solvents for spectroscopy and column chromatography were purchased through Fischer Scientific. All chemical reagents were purchased from Sigma-Aldrich and were used without further purification. Water was purified by a Millipore Milli-Q system.

Instrumentation. Absorption spectra were recorded using a Hitachi U-2800 UV−vis−NIR spectrophotometer. Room-temperature luminescence spectra were recorded using a PTI QuantaMaster spectrofluorimeter using 1 cm × 1 cm quartz cuvettes and corrected for detector sensitivity. Quartz cuvettes of 3 mm × 3 mm were used for the fluorimeter enzymatic assays. A Biotek Synergy 2 multimode microplate reader was used to record the absorbance−time trajectories for the enzyme assays. ^{1}H NMR and ^{13}C NMR spectra were recorded on a Bruker AV500 instrument at 500 and 125 MHz, respectively. Electrospray ionization (ESI) and atmospheric pressure chemical ionization (APCI) mass spectra were measured on a Bruker maXis impact. Voltammetric experiments were conducted with a computer-controlled CHI760C potentiostat.

Computational Methods. All quantum mechanical calculations were performed using the Gaussian 09 package.[31] HOMO and LUMO orbital energies were determined from the molecular geometries optimized at the B3LYP 6-31G(d) level.[58] Orbitals were visualized using the Gaussview 5 package.

Fluorescence Lifetime Studies. The fluorescence lifetime measurements were carried out using a Picoquant Fluotime 200 time-correlated single-photon-counting setup employing an LDH 470 diode laser from Picoquant as the excitation source. The laser output was at 466 nm. The excitation rate was 10 MHz, and the laser power

DOI: 10.1021/jacs.6b09735
J. Am. Chem. Soc. 2016, 138, 16388−16397

was adjusted to ensure that the detection frequency was less than 100 kHz. The laser was controlled by a PDL 88 B picosecond laser driver from Picoquant. Photons were collected at magic angle polarization.

Electrochemical Measurements. The electrochemical measurements were performed using a three-electrode system. The working electrode was a glassy carbon electrode (except for **B-VK$_{QMe_2}$**, whose CV was obtained under identical conditions but utilizing a Pt working electrode), a Pt wire was used as the counter electrode, and a Ag/$AgNO_3$ non-aqueous electrode was used as the reference. A 0.1 M solution of tetrabutylammonium hexafluorophosphate in dry or wet (10.8 M) acetonitrile was used as the electrolyte solvent, in which the dye was dissolved to 1 mM. Concentrations were determined from the absorption and calculated extinction coefficients. The solutions also contained ferrocene with a concentration of 1 mM as an internal standard. The solutions were equilibrated with argon, and all measurements were conducted under an inert atmosphere, with a minimum scan rate of 0.2 V s^{-1}. The formal redox potential was calculated from the midpoint of the cathodic and anodic peak potentials observed in the cyclic voltammograms.

Fluorescence Spectroelectrochemistry. The ITO coverslips (Evaporated Coatings Inc., 50 Ω/□; cleaned by 10 min sequential sonication in acetone, trichloroethylene, and methanol) were platinized to improve the catalytic activity of the electrode. Platinum was deposited by spin-coating 2 drops of ∼20 μL of platinum precursor solution (Plastisol T, Solaronix) on coverslips while rotating at 500 rpm. The rotation was accelerated to 2000 rpm and held at that speed for 60 s to remove excess solution. The coverslips were then sintered at 450 °C for 30 min to form the transparent platinum coating. After cooling to allow for handling, a glass tube was glued with epoxy (Hardman, McMaster-Carr) on top of the coverslip to form the sample chamber. The epoxy glue was cured by placing the samples in a 110 °C oven for ∼30 min. The sample chamber was filled with 2 mL of the desired solution (500 nM analyte, 0.1 M Bu_4NClO_4 in dry acetonitrile) and sealed by a septum pierced with the reference (AgCl-coated Ag wire) and counter (Pt wire) electrodes. Argon was bubbled through the solution for 1 h in order to deaerate the solution, and an argon-filled balloon was fixed on the sample during acquisition. The electrochemical cell was then mounted on the microscope (IX-71, Olympus). The electrochemical potential was controlled by a CHI600D electrochemical analyzer. The AgCl-coated Ag wire quasi reference electrode used was calibrated with the ferrocene/ferrocenium redox couple using $E^{\circ}_{Fc^+/Fc}$ = +0.64 V vs NHE. All potentials reported are referenced to NHE.

The laser excitation was provided by a supercontinuum laser (WhiteLase SC-400-4, Fianium, Beverly, MA). A center excitation wavelength of 515 nm was spectrally separated from the broadband emission by a computer-controlled acousto-optical tunable filter (AOTF, Fianium) and further cleaned by ET650spx and HQ517/30x excitation filters (Chroma, Rockingham, VT). A Z514-633rdc dichroic mirror (Chroma) projected the pulsed laser excitation (20 MHz repetition rate, 0.13 μW out of the objective) toward the water-immersion objective (UPLSAPO 60XW, N.A. = 1.20, Olympus). The confocal observation volume was focused 20 μm above the electrode surface, as controlled by a piezoelectric objective scanner (PIFOC P-721 controlled by an E710, Physik Instrumente (PI), Auburn, MA). The laser excitation was blocked by a 514 nm Raman notch filter, and the fluorescence emission was collected by the same objective, passed through a 50 μm diameter pinhole positioned at the image plane, and split onto two avalanche photodiode detectors (APDs; SPCM-AQR-14, PerkinElmer Optoelectronics, Vaudreuil, QC) with a 50:50 non-polarizing beamsplitter in pseudo-cross-correlation format. The data acquisition, signal from the detectors, and the piezo scanner were controlled and analyzed by software from PicoQuant (SymPhoTime).

Liposome Preparation. Aqueous solutions 20 mM in lipids were prepared as follows: 15.8 mg of DOPC was weighed in a dry vial and dissolved with a minimal amount of chloroform. The solvent was evaporated with a stream of argon while rotating the sample vial to create a thin film on the vial wall. The film was left under vacuum to remove excess solvent. After 1 h the aliquot of DOPC was hydrated with 1 mL of pH 7.4, 50 mM Tris/HCl, yielding 20 mM lipid suspensions. The lipid suspension was subjected to three freeze−thaw−sonication−vortex cycles, where each cycle involved storing the vials with the solutions in dry ice for 4 min and then thawing at 37 °C for 4 min, followed by 4 min sonication. After the third cycle, the lipid suspensions were extruded 17 times using an Avanti mini-extruder with one 100 nm polycarbonate membrane. Liposomes roughly 100 nm in diameter and each containing *ca.* 100 000 DOPC lipids were thus obtained.

In order to prepare liposomes containing the probe, the dye was extruded with the lipids to ensure proper embedding. First, 3.14 mg of DOPC was weighed in a dry vial and dissolved with a minimal amount of chloroform, and then 13.3 μL of 3 mM stock of **B-VK$_Q$** in chloroform was added to the vial. The solvent was evaporated as before to create a thin film on the vial wall and left under vacuum to remove excess solvent. The lipid−dye film was resuspended in 200 μL of buffer to give 20 mM solution of lipids containing 200 μM **B-VK$_Q$**. The same freeze−thaw−sonication−vortex cycle and extrusion steps as above were performed.

Enzymatic Assays. *Microplate Assays.* In order to test the enzymatic activity of DT-diaphorase, the NAD(P)H-dependent reduction of menadione was monitored in a coupled assay, under aerobic conditions. Reduced menadione, menadiol, in turn reduces cytochrome *c*, the absorbance of which can be followed at 550 nm (ε = 29 500 M^{-1} cm^{-1}).[59] These experiments were conducted in a well-plate reader at 37 °C. Measurements were made in 50 mM Tris/HCl pH 7.4, with 1 mg/mL (∼10 units/mL) DT-diaphorase, 200 μM NADPH (as the electron donor), 10 μM menadione (as the electron acceptor), and 30 μM cytochrome *c*. The reactions were initiated with addition of NADPH and reached a plateau after less than 1 min. The assays using the fluorogenic probe, **B-VK$_Q$**, and monitoring cytochrome *c* absorbance were conducted under the same conditions as before, where 10 μM of the probe was used. Menadione and **B-VK$_Q$** were dissolved in dimethyl sulfoxide for stock preparation due to their poor solubility in aqueous media. The final concentration of DMSO in the reaction well did not exceed 2%. Controls were also performed with the absence of enzyme, absence of probe, and absence of NADPH, as well as testing all possible combinations of the assay components to ensure only the reaction between DT-diaphorase and **B-VK$_Q$** in the presence of NADPH and cytochrome *c* gave rise to the increase in absorbance.

Fluorimeter Assays. The enzymatic reduction of **B-VK$_Q$** was also monitored via the fluorescence of the reduced probe, **B-VK$_{QH_2}$**. The system was purged with argon since the reduced probe rapidly oxidizes back to the non-emissive **B-VK$_Q$** in air. The fluorescence assays were conducted in a 3 mm × 3 mm quartz cuvette. First, 50 mM Tris/HCl buffer, 1 mg/mL (∼10 units/mL) DT-diaphorase, and 200 μM NADPH were purged with argon and added to the cuvette. The initial fluorescence intensity was recorded. An aliquot of 200 μM **B-VK$_Q$** embedded into liposomes (20 mM in lipids) was also purged with argon. Next, 7.5 μL was added to the cuvette in order to have final concentrations of 1 mM lipids and 10 μM probe. The intensity−time trajectory was then recorded for a period of 5.5 h at 1 s intervals at 37 °C. Controls were also performed without the addition of probe (only liposomes) or DT-diaphorase, or NADPH, under the same conditions.

■ ASSOCIATED CONTENT

Supporting Information

The Supporting Information is available free of charge on the ACS Publications website at DOI: 10.1021/jacs.6b09735.

Synthesis, ^{1}H NMR, ^{13}C NMR, and HRMS characterization, absorption and emission spectra of compounds, enzyme assay calculations, and control experiments, including Table S1 and Figures S1−S15 (PDF)

DOI: 10.1021/jacs.6b09735
J. Am. Chem. Soc. 2016, 138, 16388−16397

AUTHOR INFORMATION

Corresponding Author

*gonzalo.cosa@mcgill.ca

ORCID

Robert Godin: 0000-0001-7945-8548

Gonzalo Cosa: 0000-0003-0064-1345

Notes

The authors declare no competing financial interest.

ACKNOWLEDGMENTS

G.C. is grateful to the Natural Sciences and Engineering Research Council of Canada (NSERC) and the Canadian Foundation for Innovation (CFI) for funding. M.-N.B is thankful to NSERC-CGS for a graduate scholarship, R.G. is thankful to NSERC for a postgraduate scholarship, and A.M.D. is thankful to the Drug Discovery and Training Program (CIHR) at McGill for a postdoctoral fellowship.

REFERENCES

(1) Halliwell, B.; Gutteridge, J. *Free Radicals in Biology and Medicine*, 4th ed.; Oxford University Press: Oxford, UK, 2007.

(2) Murphy, M. P. *Biochem. J.* **2009**, *417*, 1.

(3) Sazanov, L. A. *Nat. Rev. Mol. Cell Biol.* **2015**, *16*, 375.

(4) Alberts, B.; Johnson, A.; Lewis, J.; Raff, M.; Roberts, K.; Walter, P. *Molecular Biology of the Cell*, 4th ed.; Garland Science, Taylor & Francis Group: New York, 2002.

(5) Kuhlbrandt, W. *BMC Biol.* **2015**, *13*, 89.

(6) Swallow, A. J. *Function of Quinones in Energy Conserving Systems*; Academic Press: San Francisco, 1982.

(7) Garcia, A. A.; Reitsma, P. H. *Vitam. Horm.* **2008**, *78*, 23.

(8) Kurosu, M.; Begari, E. *Molecules* **2010**, *15*, 1531.

(9) Vos, M.; Esposito, G.; Edirisinghe, J. N.; Vilain, S.; Haddad, D. M.; Slabbaert, J. R.; Van Meensel, S.; Schaap, O.; De Strooper, B.; Meganathan, R.; Morais, V. A.; Verstreken, P. *Science* **2012**, *336*, 1306.

(10) Arnon, D. I. *Fed. Proc.* **1961**, *20*, 1012.

(11) Manzotti, P.; de Nisi, P.; Zocchi, G. *Funct. Plant. Sci. Biotechnol.* **2008**, *2*, 29.

(12) Gong, X.; Gutala, R.; Jaiswal, A. K. *Vitam. Horm.* **2008**, *78*, 85.

(13) Stafford, D. W. *J. Thromb. Haemostasis* **2005**, *3*, 1873.

(14) Danziger, J. *Clin. J. Am. Soc. Nephrol.* **2008**, *3*, 1504.

(15) Grimm, J. B.; Heckman, L. M.; Lavis, L. D. *Prog. Mol. Biol. Transl Sci.* **2013**, *113*, 1.

(16) Nadler, A.; Schultz, C. *Angew. Chem., Int. Ed.* **2013**, *52*, 2408.

(17) Chan, J.; Dodani, S. C.; Chang, C. J. *Nat. Chem.* **2012**, *4*, 973.

(18) Miller, E. W.; Bian, S. X.; Chang, C. J. *J. Am. Chem. Soc.* **2007**, *129*, 3458.

(19) Kaur, A.; Kolanowski, J. L.; New, E. J. *Angew. Chem., Int. Ed.* **2016**, *55*, 1602.

(20) Krumova, K.; Cosa, G. In *Photochemistry*; Albini, A., Fasani, E., Eds.; Royal Society of Chemistry: Cambridge, UK, 2013; Vol. *41*, p 279.

(21) Oleynik, P.; Ishihara, Y.; Cosa, G. *J. Am. Chem. Soc.* **2007**, *129*, 1842.

(22) Khatchadourian, A.; Krumova, K.; Boridy, S.; Ngo, A. T.; Maysinger, D.; Cosa, G. *Biochemistry* **2009**, *48*, 5658.

(23) Krumova, K.; Friedland, S.; Cosa, G. *J. Am. Chem. Soc.* **2012**, *134*, 10102.

(24) Krumova, K.; Greene, L. E.; Cosa, G. *J. Am. Chem. Soc.* **2013**, *135*, 17135.

(25) Greene, L. E.; Godin, R.; Cosa, G. *J. Am. Chem. Soc.* **2016**, *138*, 11327.

(26) de Silva, A. P.; Gunaratne, H. Q.; Gunnlaugsson, T.; Huxley, A. J.; McCoy, C. P.; Rademacher, J. T.; Rice, T. E. *Chem. Rev.* **1997**, *97*, 1515.

(27) Loudet, A.; Burgess, K. *Chem. Rev.* **2007**, *107*, 4891.

(28) Wood, T. E.; Thompson, A. *Chem. Rev.* **2007**, *107*, 1831.

(29) Liu, X.-Y.; Long, Y.-T.; Tian, H. *RSC Adv.* **2015**, *5*, 57263.

(30) Lincoln, R.; Greene, L. E.; Krumova, K.; Ding, Z.; Cosa, G. *J. Phys. Chem. A* **2014**, *118*, 10622.

(31) Frisch, M. J.; Trucks, G. W.; Schlegel, H. B.; Scuseria, G. E.; Robb, M. A.; Cheeseman, J. R.; Scalmani, G.; Barone, V.; Mennucci, B.; Petersson, G. A.; Nakatsuji, H.; Caricato, M.; Li, X.; Hratchian, H. P.; Izmaylov, A. F.; Bloino, J.; Zheng, G.; Sonnenberg, J. L.; Hada, M.; Ehara, M.; Toyota, K.; Fukuda, R.; Hasegawa, J.; Ishida, M.; Nakajima, T.; Honda, Y.; Kitao, O.; Nakai, H.; Vreven, T.; Montgomery, J. A., Jr.; Peralta, J. E.; Ogliaro, F.; Bearpark, M. J.; Heyd, J.; Brothers, E. N.; Kudin, K. N.; Staroverov, V. N.; Kobayashi, R.; Normand, J.; Raghavachari, K.; Rendell, A. P.; Burant, J. C.; Iyengar, S. S.; Tomasi, J.; Cossi, M.; Rega, N.; Millam, N. J.; Klene, M.; Knox, J. E.; Cross, J. B.; Bakken, V.; Adamo, C.; Jaramillo, J.; Gomperts, R.; Stratmann, R. E.; Yazyev, O.; Austin, A. J.; Cammi, R.; Pomelli, C.; Ochterski, J. W.; Martin, R. L.; Morokuma, K.; Zakrzewski, V. G.; Voth, G. A.; Salvador, P.; Dannenberg, J. J.; Dapprich, S.; Daniels, A. D.; Farkas, Ö.; Foresman, J. B.; Ortiz, J. V.; Cioslowski, J.; Fox, D. J. *Gaussian 09*; Gaussian, Inc.: Wallingford, CT, 2009.

(32) Godin, R.; Liu, H. W.; Smith, L.; Cosa, G. *Langmuir* **2014**, *30*, 11138.

(33) Neuteboom, E. E.; Meskers, S. C. J.; Beckers, E. H. A.; Chopin, S.; Janssen, R. A. J. *J. Phys. Chem. A* **2006**, *110*, 12363.

(34) Weaver, M. J. *Chem. Rev.* **1992**, *92*, 463.

(35) Prince, R. C.; Dutton, P. L.; Bruce, J. M. *FEBS Lett.* **1983**, *160*, 273.

(36) Krumova, K.; Cosa, G. *J. Am. Chem. Soc.* **2010**, *132*, 17560.

(37) Hui, Y.; Chng, E. L.; Chng, C. Y.; Poh, H. L.; Webster, R. D. *J. Am. Chem. Soc.* **2009**, *131*, 1523.

(38) Aguilar-Martínez, M.; Macías-Ruvalcaba, N. A.; Bautista-Martínez, J. A.; Gómez, M.; González, F. J.; González, I. *Curr. Org. Chem.* **2004**, *8*, 1721.

(39) Gupta, N.; Linschitz, H. *J. Am. Chem. Soc.* **1997**, *119*, 6384.

(40) Cannes, C.; Kanoufi, F.; Bard, A. J. *Langmuir* **2002**, *18*, 8134.

(41) Mack, D. O.; Wolfensberger, M.; Girardot, J. M.; Miller, J. A.; Johnson, B. C. *J. Biol. Chem.* **1979**, *254*, 2656.

(42) Bovicelli, P.; Borioni, G.; Fabbrini, D.; Barontini, M. *Synth. Commun.* **2008**, *38*, 391.

(43) Heineman, W. R. *J. Chem. Educ.* **1983**, *60*, 305.

(44) Palacios, R. E.; Chang, W. S.; Grey, J. K.; Chang, Y. L.; Miller, W. L.; Lu, C. Y.; Henkelman, G.; Zepeda, D.; Ferraris, J.; Barbara, P. F. *J. Phys. Chem. B* **2009**, *113*, 14619.

(45) Yilmaz, I. *Transition Met. Chem.* **2008**, *33*, 259.

(46) Pinyayev, T. S.; Seliskar, C. J.; Heineman, W. R. *Anal. Chem.* **2010**, *82*, 9743.

(47) Godin, R.; Cosa, G. *J. Phys. Chem. C* **2016**, *120*, 15349.

(48) The enhancement is calculated after the fluorescence intensity–time trajectory of B-VKQ in the presence of acid under applied bias has been subtracted by that of the blank electrolyte solution.

(49) Iyanagi, T.; Yamazaki, I. *Biochim. Biophys. Acta, Bioenerg.* **1970**, *216*, 282.

(50) Cui, K.; Lu, A. Y.; Yang, C. S. *Proc. Natl. Acad. Sci. U. S. A.* **1995**, *92*, 1043.

(51) Tedeschi, G.; Chen, S.; Massey, V. *J. Biol. Chem.* **1995**, *270*, 1198.

(52) Berman, H. M.; Westbrook, J.; Feng, Z.; Gilliland, G.; Bhat, T. N.; Weissig, H.; Shindyalov, I. N.; Bourne, P. E. *Nucleic Acids Res.* **2000**, *28*, 235.

(53) Faig, M.; Bianchet, M. A.; Talalay, P.; Chen, S.; Winski, S.; Ross, D.; Amzel, L. M. *Proc. Natl. Acad. Sci. U. S. A.* **2000**, *97*, 3177.

(54) Rajagopal, B. S.; Edzuma, A. N.; Hough, M. A.; Blundell, K. L.; Kagan, V. E.; Kapralov, A. A.; Fraser, L. A.; Butt, J. N.; Silkstone, G. G.; Wilson, M. T.; Svistunenko, D. A.; Worrall, J. A. *Biochem. J.* **2013**, *456*, 441.

(55) Qian, Y.; Karpus, J.; Kabil, O.; Zhang, S. Y.; Zhu, H. L.; Banerjee, R.; Zhao, J.; He, C. *Nat. Commun.* **2011**, *2*, 495.

(56) Träuble, H.; Overath, P. *Biochim. Biophys. Acta, Biomembr.* **1973**, *307*, 491.

DOI: 10.1021/jacs.6b09735
J. Am. Chem. Soc. 2016, 138, 16388–16397

(57) Schlamadinger, D. E.; Gable, J. E.; Kim, J. E. *J. Phys. Chem. B* **2009**, *113*, 14769.
(58) Mendez-Hernandez, D. D.; Tarakeshwar, P.; Gust, D.; Moore, T. A.; Moore, A. L.; Mujica, V. *J. Mol. Model.* **2013**, *19*, 2845.
(59) van Gelder, B. F.; Slater, E. C. *Biochim. Biophys. Acta* **1962**, *58*, 593.

DOI: 10.1021/jacs.6b09735
J. Am. Chem. Soc. 2016, 138, 16388−16397